Biochemistry and Biophysics Reports 41 (2025) 101945

Contents lists available at ScienceDirect

Biochemistry and Biophysics Reports

journal homepage: www.elsevier.com/locate/bbrep

Oxidative impact on lipoprotein structure: Insights from dynamic light scattering

Nickolette Kong [a], Natalia Penaloza [a], Gustavo Agreda [a], Angela B. Nguyen [a], Joseph Gutheinz [b,a], Alison Tran [a], Nhi Nguyen [a], Tuong Vi Ho [a], Ana Marin [a], Birgit Mellis [b], Richa Chandra [a,*]

[a] University of St. Thomas, Department of Chemistry and Biochemistry, 3800 Montrose Blvd, Houston, TX, 77006, USA
[b] University of St. Thomas, Department of Physics and Engineering, 3800 Montrose Blvd, Houston, TX, 77006, USA

ARTICLE INFO

Keywords:
Lipoprotein
Peroxidation
Nitration
Oxidation
Dynamic light scattering
Cardiovascular disease

ABSTRACT

Cardiovascular disease (CVD) is the number one cause of mortality worldwide, with oxidative stress contributing significantly to its pathogenesis. Lipoproteins, key biomolecules in lipid transport, are particularly susceptible to oxidative modifications, which can contribute to atherogenesis. The need for advanced analytical tools to better understand the pathogenesis of cardiovascular disease (CVD) is critical due to its significant impact on public health. Clinicians often rely on indirect calculations of low-density lipoprotein (LDL) as a primary diagnostic indicator, which can oversimplify and overlook the complex changes in lipoprotein structure and function and therefore the complex etiology of CVD. Here it is demonstrated that dynamic light scattering (DLS) is sensitive and effective at measuring variation in lipoprotein size distributions following oxidative damage caused by peroxidation and nitration—two common physiological processes that play dual roles in both normal and pathogenic states. We establish the utility of DLS in detecting subtle variations in lipoprotein size, including potential aggregation and fission events resulting from chemical modifications. Our work highlights the value of DLS in advancing our understanding of the pathogenic mechanisms underlying CVD development, while also providing a foundational framework to study other biological processes and their effects on lipoproteins, ultimately guiding the development of therapies to address these harmful processes.

1. Introduction

According to the 2024 statistical update from the American Heart Association, it is estimated that almost half of American adults ≥20 years old are affected by some form of cardiovascular disease (CVD). Among the top 20 risk factors for a year of life lost and death from CVD are smoking, alcohol use, diets low in fruits and vegetables, and diets that are high in red or processed meat. Electronic cigarette use is potentially an emergent CVD risk factor as well, though the long-term risks are not understood yet. Electronic cigarettes as well as electronic hookah flavored vaping correlate to higher levels of cardiovascular injury biomarkers most likely due to oxidative stress [1]. As such, there is a strong correlation of higher oxidative stress due to diet and lifestyle and the development of CVD. This data points to the importance of understanding the relationship of higher oxidative stress and the development of CVD. It is also crucial to investigate the molecular-level relationships to identify the chemical processes responsible for structural changes like lipoprotein aggregation and fission. Understanding these mechanisms is essential for developing pharmaceutical therapies to prevent such reactions [2].

Lipoproteins are highly heterogeneous biomolecules comprised of proteins and lipids including triglycerides, cholesterol, and phospholipids. These particles circulate in blood and transport lipids. The three main classes include HDL (high density lipoproteins), LDL (low density lipoproteins), and VLDL (very low-density lipoproteins) (Fig. 1) [3].

HDL comes from the liver and is responsible for the return of

Abbreviations: DLS, dynamic light scattering; CVD, cardiovascular disease; HDL, high density lipoprotein; LDL, low density lipoprotein; VLDL, very low density lipoprotein; ox-LDL, oxidized LDL; LDL-C, LDL-cholesterol; ROS, reactive oxygen species; RNS, reactive nitrogen species; sdLDL, small dense LDL; PSD, particle size distribution.

* Corresponding author.
E-mail address: chandrr@stthom.edu (R. Chandra).

https://doi.org/10.1016/j.bbrep.2025.101945
Received 21 October 2024; Received in revised form 26 January 2025; Accepted 5 February 2025

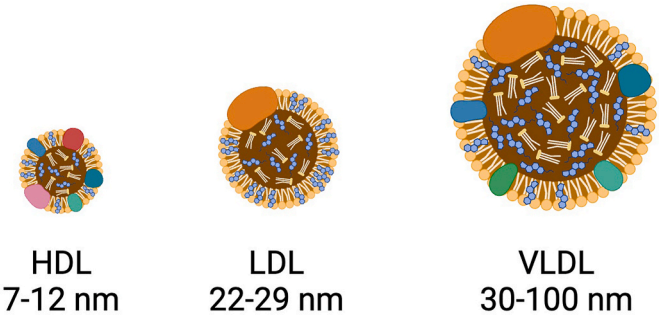

Fig. 1. The three main classes of lipoproteins with typical size ranges visualized with a core of triacylglycerols and cholesterol esters, a phospholipid membrane with free cholesterol and embedded proteins. Created with BioRender.com.

cholesterol to the liver from peripheral tissue, a process called reverse cholesterol transport. Unlike LDL and VLDL, HDL is known to be anti-atherogenic potentially through obstruction of LDL oxidation. HDL, the smallest and most dense of the main lipoproteins, range in size from 7 to 12 nm with the highest percentage of protein content and the lowest amount of lipids [4,5].LDL has higher lipid content than HDL. Its normal physiological function is cholesterol delivery from the liver to peripheral tissues. LDL ranges from 22 to 29 nm in diameter and includes several subclasses including small dense and large buoyant forms. Some forms of LDL are small enough to become trapped in the inner lining of arteries, which potentially leads to oxidation and buildup of plaque [6]. VLDL is a precursor to LDL and is also considered atherogenic. VLDL is the most lipid rich of the main classes and comprise a broader diameter range of 30–100 nm [7]. All three of the lipoprotein classes are involved in a sequential metabolic process of delipidation with triglycerides being the main lipid lost. As such, there is greater diversity in the triglyceride-rich subclasses, which include VLDL, and it is difficult to distinguish discrete subfractions [8].

As aforementioned, oxidative stress, which forms excess reactive oxygen species (ROS) and reactive nitrogen species (RNS), is physiologically relevant to the mechanisms behind CVD development. On the other hand, ROS and RNS have normal and essential functions for cells and other biological processes. For example, hydrogen peroxide (H_2O_2), an ROS, is involved in the maintenance of normal vascular function. However, uncontrolled amounts of H_2O_2 induce peroxidation of lipids which alters lipoproteins enough to trigger inflammation and arterial damage [9]. Nitric oxide (NO•) is an RNS with normal physiological functions in vascular signaling. Conversely, uncontrolled production of nitric oxide can lead to vascular injury [9]. When nitric oxide is in excess, it is hypothesized that complex *in vivo* biochemical reactions take place in the development of atherosclerosis. Nitric oxide is rapidly oxidized into its stable form, nitrite (NO_2^-), which accumulates in phagocytes. This nitrite buildup is commonly used as an indicator of nitric oxide production. In addition, myeloperoxidase, a cellular enzyme of the immune system, acts as a catalyst to facilitate the reaction of hydrogen peroxide and chloride ions to generate hypochlorous acid (HClO). HClO is a known precursor to free radicals in the body. Hypochlorous acid (HClO) and nitrite (NO_2^-) undergo a redox reaction to form nitrate ion (NO_3^-) (Fig. 2). The transfer of the oxygen from HClO to NO_2^- is hypothesized to form nitryl chloride Cl–NO_2 as a transitory intermediate that can nitrate and chlorinate lipoproteins [10,11].

In this report, we examine modifications of lipoprotein size distributions measured by DLS following the two nonenzymatic chemical reactions described above. DLS has been proven effective in measuring nuanced differences in size distributions for various lipoproteins in human blood including small dense LDL and large LDL [12]. In addition, we previously reported on a combinatorial immunoassay approach with DLS to characterize specific proatherogenic lipoproteins known as remnant lipoproteins (RLP) in 2016 [13].

Traditionally, DLS is powerful at determinizing the hydrodynamic particle size of nanoparticles in a colloidal solution. This technique has applications in Materials Science [14,15] and also in various areas of Physics, Chemistry, and Biology [16]. In recent years, the dynamic light scattering method found more and more uses in the biomedical sciences [17], including measuring the size distribution of nanoparticles for studies on cell nanotoxicity [18] or feasibility studies of performing quantitative measurements of sdLDL cholesterol for clinical studies [19]. DLS has additionally been utilized for other aspects of lipoprotein biochemistry but this research has so far been limited to human models most likely due to the clinical relevance of lipoprotein sizing [12,13, 20–23]. However, the methodology may be applicable to other animal models based on the principles of DLS described here.

The concepts and theoretical foundations of DLS are well established [24–26]. In this instrument, laser light is backscattered by nanoparticles in the solution. The instrument also contains a detector that is coupled with a time - correlated photon counter. This detector measures the backscattered light in frequent intervals over a short time. The data is compiled into a single measurement, capturing the speed at which the backscattered light intensity varies during the specific time period. The intensity varies due to random particle movement (Brownian motion) in the aqueous solution (here 0.05 mM tris-HCl, pH 7.4). This diffusion results in fluctuations in the local concentration of particles and therefore in a continuous change of the interference pattern of the backscattered light by those particles at the detector, resulting in varying intensity measurements. The local concentration of particles is constantly varying due to the random particle movement. This results in continuous alteration of the intensity measurements. As such, the periods of intensity fluctuations and particle motion correspond to each other. Since the Brownian motion of the particles is influenced by the diffusion coefficient (D), the variations in the intensity of the backscattered light are utilized by the software to calculate the hydrodynamic size of the particles. Larger particles move more slowly through a solution and therefore have a smaller diffusion coefficient. Particles that are larger diffuse slower and result in a smaller value for the diffusion coefficient. The software derives the particle radius (r) through the measured diffusion coefficient based on the Einstein Stokes relationship: $D = kT/6\pi\eta r$ (with η = Viscosity of solvent, k = Boltzmann constant, T = Temperature in Kelvin).

When evaluating DLS measurements of polydisperse, small particle or dilute solutions, such as lipoproteins, caution must be taken to decide on the proper analysis method and interpretation of data to receive reliable and reproducible measurements [27]. Modifications are required in polydisperse solutions since larger particles scatter more light than smaller ones, which means that a small number of large particles can overshadow the measurement of a significant number of smaller particles [28]. This can skew the proportion of the size distribution toward the larger particles and, in some cases, may entirely

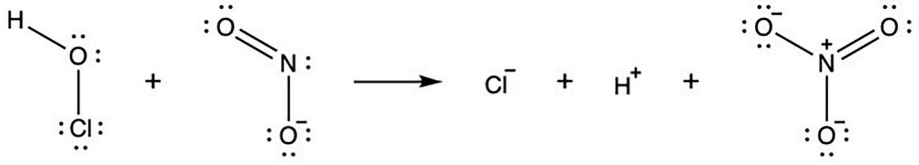

Fig. 2. Overall reaction of hypochlorous acid (HOCl) and nitrite ion (NO_2^-)

conceal the smaller particles. The intensity-based size distributions must be adjusted for the light intensity contributed by each population of particle sizes, leading to a derived volume-based size distribution. These derivations are based on Mie Theory [29–31] in which the refractive index, particle size, and scattering angle to the intensity of scattered light are related. In this work, these computations are automatically performed by the instrument's software (Malvern Zetasizer Nano S) and are presented as the Volume Particle Size Distributions (Volume PSDs) discussed in the results section.

Building on our previous work, we leverage DLS as a precise and sensitive method to explore the intricate changes in lipoprotein size distributions under oxidative conditions. By applying DLS to measure the effects of specific chemical modifications on lipoproteins, we aim to advance our understanding of CVD pathogenesis. In this report, we showcase DLS as a novel bioanalytical tool for elucidating the alterations in size distributions of HDL, LDL, and VLDL induced by chemical modifications, thereby enhancing our comprehension of their role in CVD.

2. Materials and Method

2.1. Materials

Commercial HDL (Cat No. 361-10, Lot Number 12C1847), LDL (Cat No. 360-10, Lot Number 03C1863), and VLDL (Cat No. 365-10, Lot Number 11C1054) standards were purchased from Lee Biosolutions. Lipoprotein standards are negative for HIV and other infectious agents. No further identifying information is provided aside from cholesterol and triglyceride concentrations. Sodium nitrite (97.0 %, Product No. 237213), hydrogen peroxide (Product No. 216763), phosphate buffer solution (0.1 M, Product No. P5244), sodium chloride (Product No. S7653), sodium perchlorate (98 %, Product No. 000090), EDTA Disodium salt Dihydrate (Product No. 324503), and sodium hypochlorite (Product No. 425044) were all purchased from the Sigma-Aldrich company. TBARS (TCA Method) Assay Kit (Product No. 700870) was purchased from Caymen Chemical, Ann Arbor, MI. The clinical serum sample was purchased from Discovery Life Sciences (Product Number: DLS16-79964). The sample is from a 46 year old female with no further identifying information. The clinical result for this sample provided by the company was a 745 mg/dL triglyceride value obtained by Siemens-Advia 2400 on Nov. 8, 2016. The clinical sample is stored at −80 °C for long term storage. The LDL/VLDL and HDL Purification Kit (Ultracentrifugation Free, Catalog No. STA-608) was purchased from Cell Biolabs, Inc., San Diego, CA.

2.2. Lipoprotein preparations

The cholesterol and triglyceride values for each lipoprotein standard, which were provided by Lee Biosolutions, are summarized in Table 1. Protein concentrations for each lipoprotein standard were determined in laboratory through a standard Bradford Analysis and are also listed in Table 1. In addition, Certificates of Analysis for each are provided in the Supplementary materials (Supplemental File 1. COA of Lipoproteins). The lipoprotein samples are pooled from multiple individuals and then purified by ultracentrifugation. As such, there is a higher diversity in sizes in our control samples prior to chemical modification.

Table 1
Chemical information of lipoprotein standards (Lee Biosolutions).

	HDL	LDL	VLDL
Total Cholesterol (mg/dL)	3120	5130	3360
Lipoprotein Cholesterol (mg/dL)	2920	3620	Not provided
Triglycerides (mg/dL)	1300	3160	11,740
Protein (mg/mL)[a]	93	26	45

[a] Protein concentration determined in laboratory through a standard Bradford Analysis.

Lipoproteins (LDL, HDL, and VLDL), both controls and chemically modified, were prepared in 0.15 M NaCl to simulate physiological levels as described elsewhere [32]. Lipoprotein controls not intended for chemical modification were also prepared with 0.01 mM EDTA to prevent further oxidation than the level that is expected from exposure to air [33]. In addition, as stated above, no further identifying information including gender or age of the individuals from which the samples were acquired is provided by the vendor, and we are limited to the values provided and the values determined in our laboratory as listed in Table 1.

Lipoproteins were prepared at protein concentrations to match our previous work, in which we demonstrated the ideal values that correspond to physiological concentrations which resulted in reproducible DLS measurements [13]. Briefly, LDL was diluted at a 1 % (v/v) dilution in reagent solution (dependent on the mechanism described below). The final protein concentration of 0.26 mg/mL was targeted to match our previous work to ensure reproducibility in the DLS measurements. VLDL was prepared under the same criterion at a target protein concentration of 0.022 mg/mL to match our previous work [13]. As such, VLDL was prepared at 0.05 % (v/v) dilution in the reagent solutions. As we have not examined HDL previously, it was prepared at a target physiological value of 47 mg/dL of total cholesterol, which is comparable to the total cholesterol (51 mg/dL) value for LDL. HDL was prepared at a 1.5 % (v/v) dilution in the reagent solutions. This HDL preparation resulted in a protein concentration of 1.39 mg/mL, HDL cholesterol of 44 mg/dL, and triglyceride concentration of 20 mg/dL.

2.3. Peroxidation of lipoproteins

Three separate controls of HDL, LDL and VLDL with the concentrations described above in 0.15 M NaCl, 0.01 mM EDTA were incubated for 24 h at 37 °C as a comparison to peroxidation samples. It is important to note that the concentration of hydrogen peroxide used in this study is substantially higher than that observed *in vivo*, where processes like apoptosis, tumor development, and necrosis involve hydrogen peroxide concentrations in the micromolar range—approximately 1000 times lower than the concentration applied here [34]. Nonetheless, the lipoproteins were prepared as described elsewhere, exposed to 0.3 % hydrogen peroxide, and incubated at 37 °C for a period of 24 h. This approach follows established laboratory protocols for inducing peroxidation in a controlled setting to study oxidative effects [35]. To confirm effective conjugated diene production from the peroxidation of lipids, the absorbance at 234 nm was measured both before and following the 24-h incubation, which is conventional for chemical oxidation assays of lipid containing biomolecules [7,10,35,36]. In addition, TBARS (thiobarbituric acid reactive substances) assays was employed as a complement to the measurement of conjugated dienes to further confirm the effect of the peroxidation and nitration reactions. The TBARS assay is generally used as a measure of oxidative stress in biological samples as the reaction mechanism involves the reaction of thiobarbituric acid (TBA) to malondialdehyde (MDA), which is a direct product of lipid peroxidation. This adduct forms a pink color that can be quantified colorimetrically or fluorometrically [37]. In this work, we measured all lipoproteins at 0 h and at 24 h following incubation fluorometrically at an excitation of 530 nm and emission of 550 nm as described in the kit manual.

2.4. Nitration of lipoproteins

Lipoproteins undergoing the second chemical reaction of nitration were incubated at 37 °C for a period of 24 h in the same manner as the peroxidation samples. Controls were also prepared as above in 0.15 mM NaCl and 0.01 mM EDTA. The lipoproteins undergoing the nitration were prepared at the same resultant concentrations but with different reagents and buffer to control for pH for this mechanism. For example, 10 μL of LDL was added to 970 μL of 0.15 M NaCl in 10 mM PBS (pH of

7.4). Then 10 μL of 20 mM $NaNO_2$ was added followed by 10 μL of 20 mM NaOCl. The order of these steps and pH control were critical to ensure formation of HClO (pKa 7.5), which is required for the mechanism [10,38]. Again, conjugated diene production was measured via absorbance at 234 nm following the 24-h incubation, and TBARS assays were performed both prior to and after the reaction.

2.5. Size distributions of lipoproteins via dynamic light scattering

We acquired size distributions for all controls and samples by volume and intensity through the Malvern DLS instrument. We employed the Zetasizer Nano S from Malvern Instruments as our DLS instrument, which features a 632.8 nm laser light source and a maximum measurement angle of 175°. The detectable particle size range spans from 0.3 nm up to 10 μm. For the lipoprotein measurements, the following key parameters were selected: sample viscosity, temperature, refractive index, absorbance, equilibration time, and dispersant as described before [13].

Briefly, the samples were heated to 35 °C, equilibrated for 120 s, and the sample viscosity was set to 0.7138 cP, as the standards are diluted in their respective aqueous matrices. Also, the refractive index for our samples (highly diluted in aqueous medium) was obtained using a Cole-Palmer digital refractometer at 1.336 (at 25 °C). The absorbance was measured at 0.200 at visible wavelengths (450 nm and 530 nm). Each sample was subjected to two measurements providing average particle diameter values for different peaks along with their relative percentages. Each value consists of data collected continually over a 3–5-min period. These parameters were maintained from our previous work to ensure valid comparison [13].

The software displays Intensity Particle Size Distributions (Intensity PSD) and Volume PSD, which we presented in our previous work [13]. Volume PSDs like Intensity PSDs are generated from the same measured values but are adjusted to account for the impact due to disparate particle sizes. We compare the Volume PSDs for the peroxidation and nitration reactions in our discussion. When examining the change from the Intensity PSDs to the Volume PSDs, the size positions for the peaks decrease. In the Volume PSDs, the peak heights are valuable for estimating the relative amounts of particles with distinctive sizes. In contrast, Intensity PSDs are not suitable for discerning relative contributions due to a masking effect of larger sized particles, which backscatter more light. The rationale and process for the above calculations are described in the ISO document as 13321:1996 E and 22412.

2.6. Feasibility of lipoprotein preparations from a clinical sample

We demonstrate the feasibility of performing size distribution analysis using DLS on a single donor clinical sample. The sample is from a 46-year-old female with a triglyceride level of 745 mg/dL. LDL and VLDL were separated from HDL using the LDL/VLDL and HDL Purification Kit (Cell Biolabs, Inc.) according to the manufacturer's protocol and as described elsewhere [39]. Adjustments were made to the assay volumes provided by the manufacturer to accommodate the 1 mL serum sample volume.

Following the initial HDL purification, VLDL was isolated from LDL through ultracentrifugal flotation in 0.15 M NaCl (density <1.006 g/mL). Specifically, 1 mL of 0.15 M NaCl was layered over the LDL/VLDL mixture and ultracentrifuged at 120,000 rpm for 1 h and 40 min at 4 °C, using the TLA 120.2 fixed-angle rotor in the Optima XP Beckman Ultracentrifuge. After ultracentrifugation, the top 500 μL layer containing VLDL was carefully aspirated, separating it from LDL.

All three lipoprotein fractions were concentrated to approximately 50 μL using Nanosep 100 K Omega filters (Pall Corporation, Ann Arbor, Michigan), which have nominal pore sizes of 10 nm. This step served to remove residual albumin and concentrate the samples for DLS analysis. Protein concentrations of HDL, LDL, and VLDL were measured using the Protein A280 Application on Thermo Scientific's NanoDrop One Spectrophotometer, yielding values of 4.180 mg/mL, 0.024 mg/mL, and 0.039 mg/mL, respectively. Each sample was then diluted to a final volume of 500 μL with 0.15 M NaCl to meet the minimum sample volume required for DLS analysis. The prepared samples were analyzed using DLS to obtain Volume PSDs, as described above in Section 2.5.

3. Results and Discussion

3.1. Conjugated diene formation following oxidation at 234 nm

Based on absorbance values taken after 24 h incubation, conjugated diene production was higher in both peroxidized and nitrated lipoproteins compared to their respective controls as shown in Table 2. There is intrinsic conjugated diene production in the controls as well since they were exposed to air prior to the addition of the EDTA. The relative increase in absorbance and hence conjugated diene concentration is more pronounced in LDL than HDL, and even more so in VLDL samples which have the highest concentration of lipids. Peroxidation of VLDL yields a dramatic increase which can also be attributed to the higher concentration of triglycerides (Table 1) compared to both LDL and HDL. As such, VLDL has the highest susceptibility to peroxidation and conjugated diene formation out of all lipoproteins in the fasting state. The results here also prove that peroxidation produces a greater concentration of conjugated dienes than the nitration reaction. Nitration does not have as profound of an effect on conjugated diene production as the biochemical pathway for the reaction does not involve free radical lipid peroxide formation [10,11].

3.2. Estimation of lipid peroxidation via TBARS assay

TBARS assays provided additional results including initial oxidation status of the lipoprotein samples as well as following the nitration and peroxidation reactions (Table 3).

Human serum from normal healthy individuals has an MDA concentration between 1.80 and 3.94 μM when measured through the TBARS assay at 532 nm colorimetrically. When serum is exposed to oxidizing conditions chemically, its concentration can increase 6 to 7 times [40]. Across all three lipoprotein classes (HDL, LDL, and VLDL) which were prepared at physiological concentrations, MDA levels, used as an indicator of lipid peroxidation, remained relatively stable in control samples during the 24-h incubation period with only HDL being in the normal range seen in other studies. This consistency suggests that the lipoproteins possessed a baseline level of oxidation prior to the assay, likely due to their exposure to oxidizing conditions before the addition of EDTA.

The addition of 0.3 % hydrogen peroxide (H_2O_2) to induce peroxidation resulted in increased MDA levels for LDL and VLDL, with VLDL exhibiting the most significant rise. This observation aligns with the data from Table 2, showing VLDL's greater susceptibility to oxidative stress, evidenced by its marked increase in conjugated diene production following peroxidation. Interestingly, HDL exhibited minimal change in MDA levels under these conditions, reflecting its comparatively lower susceptibility to lipid peroxidation.

The nitration reaction led to a notable increase in MDA levels for LDL, both at the initiation of the assay and after 24 h of incubation. LDL exhibited the highest MDA concentration under nitration conditions, while VLDL showed a moderate rise, and HDL maintained comparatively lower levels.

Table 2
Absorbance at 234 nm ± CV following 24-h incubation at 37 °C.

Lipoprotein Class	Control	Peroxidation	Nitration
HDL	0.290 ± 3 %	0.331 ± 3 %	0.314 ± 2 %
LDL	0.223 ± 6 %	0.288 ± 3 %	0.253 ± 4 %
VLDL	0.370 ± 0.5 %	2.640 ± 0.7 %	0.532 ± 0.6 %

Table 3
Estimation of MDA (μM) ± CV measured by TBARS Assay at 0- and 24-h Incubation at 37 °C.

Lipoprotein Class	Control		Peroxidation		Nitration	
	0 Hour	24 Hour	0 Hour	24 Hour	0 Hour	24 Hour
HDL	2.5 ± 3 %	2.4 ± 1 %	2.1 ± 7 %	2.7 ± 0.3 %	4.0 ± 1 %	3.4 ± 1 %
LDL	8.0 ± 3 %	6.7 ± 4 %	2.2 ± 0.1 %	5.0 ± 0.2 %	16.7 ± 2 %	15.7 ± 0.1 %
VLDL	6.9 ± 1 %	7.9 ± 1 %	27.9 ± 1 %	37.7 ± 2 %	6.5 ± 1 %	10.7 ± 1 %

Additionally, an orange coloration was observed in samples subjected to peroxidation reflecting the reaction TBA with MDA and other aldehydes generated during lipid oxidation. It is known that many different monofunctional aldehydes are produced from oxidation of lipids and the TBA reaction with these other aldehydes can produce yellow and orange pigments as well [41]. While our fluorescence measurements focused on red pigments measured at 535 nm, the presence of yellow and orange hues suggests the contribution of other aldehydes in the peroxidation reactions. Thus, the results emphasize the distinct oxidative and nitrative susceptibilities of the lipoprotein classes, with VLDL demonstrating heightened sensitivity to peroxidation and LDL showing a strong response to nitration mechanisms.

3.3. Size distributions of lipoproteins via dynamic light scattering

Due to the polydisperse nature of native VLDL and the increase in polydispersity following the chemical reactions of LDL and VLDL, we evaluated the shifts in size distributions by volume in this study. This gives us more precise results than evaluation by intensity distribution which will mask contributions by smaller particles as mentioned earlier. HDL appears to be robust to both peroxidation and nitration presenting single peaks and monodisperse results (Fig. 3, Table 4). HDL is the most monodisperse subtype when measured by diameter as seen in the examples of size distributions for HDL control and HDL samples following peroxidation and nitration.

Table 4
Volume PSD of HDL: Mean Diameter ± SD (nm) (Relative % of Populations), n = 10.

Control	11.3 ± 0.3 (100 %)
Peroxidation	11.9 ± 0.3 (100 %)
Nitration	11.6 ± 0.2 (100 %)

In addition, the volume PSDs display consistent distributions of HDL under both reaction conditions (Fig. 3). HDL exhibits small standard deviations of less than 1 nm which indicates that it is monodisperse (one size population) despite peroxidation or nitration. Though HDL subtypes can be measured through other methods that distinguish slight differences in protein isoforms and densities [42,43], DLS, as we have shown before [13], provides a highly precise diameter result.

The volume PSDs for LDL reveal profound changes following peroxidation and nitration. In Fig. 4, three representative DLS Volume PSDs are shown as an example of the data that is enumerated in Table 5. Three unique populations of LDL particles are observed. The relative percentage and in some cases the diameter of the populations for both the peroxidation and nitration mechanisms shift compared to the control populations. Among the three populations in the control, the smallest LDL is the most abundant (96 ± 2 %) with a mean diameter of 31 ± 1 nm. Following peroxidation and nitration, this population (31 ± 3 nm) decreases to a relative percentage of 89 ± 7 % and 80 ± 1 % respectively

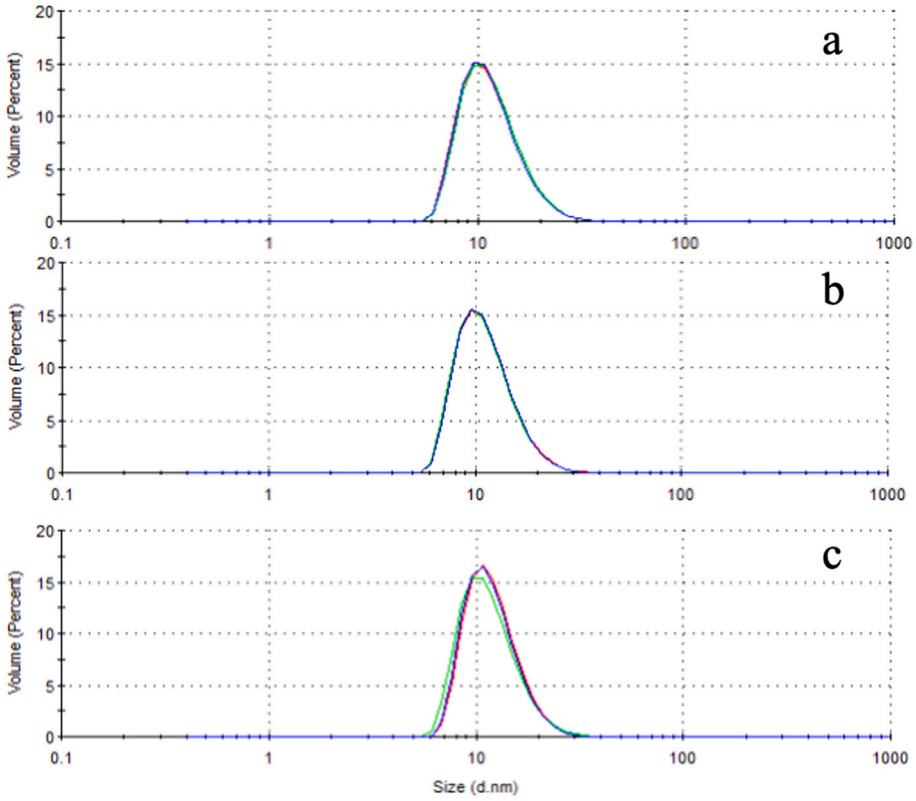

Fig. 3. Examples of Volume PSDs Measured by DLS for HDL Samples: a) Control, b) Peroxidation, and c) Nitration

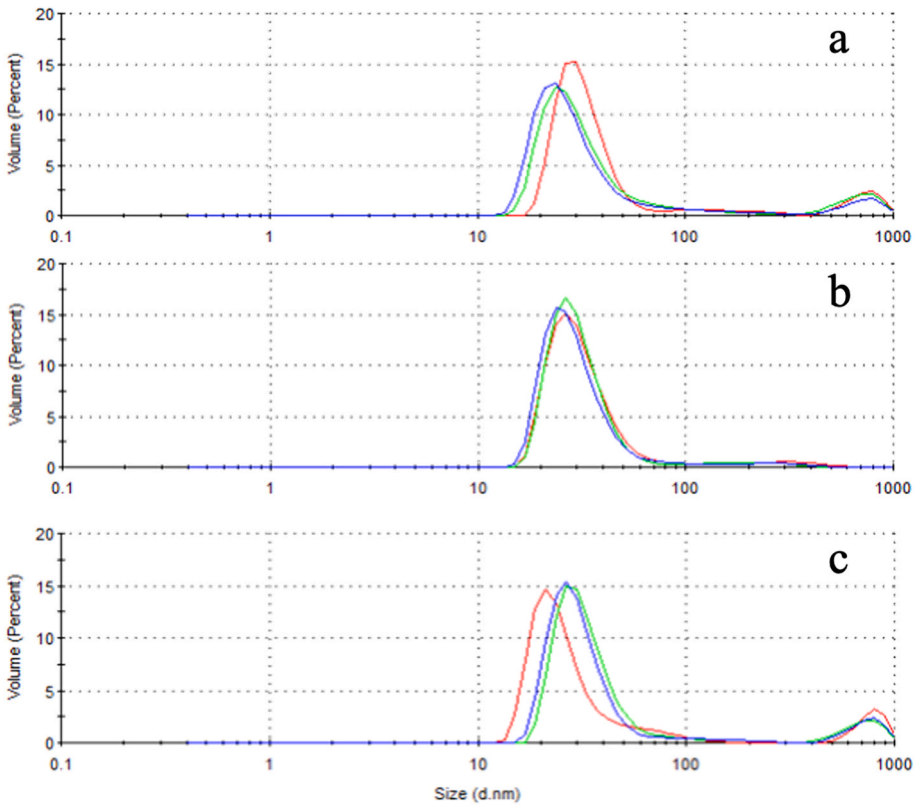

Fig. 4. Examples of Volume PSDs Measured by DLS for LDL Samples: a) Control, b) Peroxidation, and c) Nitration

Table 5
Volume PSDs of LDL: Mean Diameter ± SD (nm) (Relative % of Populations), n = 10.

	Population 1	Population 2	Population 3
Control	31 ± 1 (96 ± 2 %)	314 ± 159 (3 ± 2 %)	589 ± 185 (1 ± 2 %)
Peroxidation	31 ± 3 (89 ± 7 %)	162 ± 119 (4 ± 3 %)	696 ± 74 (9 ± 5 %)
Nitration	29 ± 4 (80 ± 1 %)	104 ± 25 (4 ± 3 %)	747 ± 34 (15 ± 3 %)

but generally maintains diameters close to the control value. The largest sized population in LDL measures at a mean diameter of 589 ± 185 nm and a relative percentage of 1 ± 2 %. Following peroxidation, this population increases in diameter to 696 ± 74 nm and a relative percentage at 9 ± 5 %. This change is more prominent with the nitration mechanism resulting in a diameter increase to 747 ± 34 nm and an increased relative percentage of 15 ± 3 %.

The shifts towards populations with larger volume PSDs indicate aggregation following chemical oxidation. Oxidation of LDL is known to produce LDL aggregates measured by neutron scattering and turbidity experiments [44,45]. Upon aggregation, a decrease in the native LDL population takes place with the formation of LDL oligomers [44]. In the LDL control since 96 ± 2 % of the population has a volume PSD of 31 ± 1 nm, we use that as a reference to compare the shifts in the larger populations following peroxidation and nitration reactions. With peroxidation, a population of LDL appears that is 162 ± 119 nm. Comparing the lower end and higher end of this population to the native LDL of the control, we hypothesize that we have an average of 5 LDL particles aggregating (5 × 31 nm = 155 nm). The data points to 1 to 9 LDL particles oligomerizing in this population based on the range. The largest population (696 ± 74 nm) which makes up a more significant proportion of the particles detected by volume following peroxidation, may be comprised of 20–25 native LDL particles aggregating at an average of 23 particles. Nitration produces different aggregation patterns. The second largest population that appears is smaller than in the peroxidation reaction at 104 ± 25 nm, which indicates that this population consists of 3–4 LDL particle oligomers. A substantial proportion of the volume PSD is derived from the largest population of LDL following nitration at 15 % and a larger diameter of 747 ± 34 nm. This group may be populated by aggregates of 23–25 LDL particles. Neutron and X-Ray scattering have been previously used examine the polydispersity of LDL in solution. Through neutron scattering, the effects of Cu^{2+} based oxidation on LDL shows that LDL can double in size and produce dimers and trimers and continuously aggregate to even larger oligomers. After 30 h, LDL is no longer spherical forming aggregates without a distinct structure, and the main surface protein on the particle, apolipoprotein B-100 (apoB-100), undergoes fragmentation continuously through the oxidation period [44,46].

Volume PSDs for VLDL reveal some similar trends. Fig. 5 illustrates this with three example DLS Volume PSDs as visual aids for the data in Table 6. VLDL, as a biomolecule comprised of mainly triglycerides, is more diverse in size in its native state due to its complex assembly and metabolic modifications after secretion by the liver [47]. Again, in our work, three populations of VLDL are detected by volume in all samples.

Most of the control VLDL falls within the expected diameter range of native VLDL (30–100 nm) [7,48] at a mean diameter of 66 ± 14 nm and is a monomeric species. The two other larger populations are detected at lower relative percentages around 26 % and arise from larger particles in the sample and aggregates from oxidation effects within the control sample as evidenced by the TBARS measurement of MDA (Table 3). In this report, we emphasize the relative changes observed between the control sample and those subjected to peroxidation and nitration. As such, the monomeric VLDL population, which most closely resembles native VLDL, shows an increase in average diameter following both biochemical modifications. With peroxidation, VLDL increases to an average diameter of 73 ± 24 nm and decreases to a relative percentage

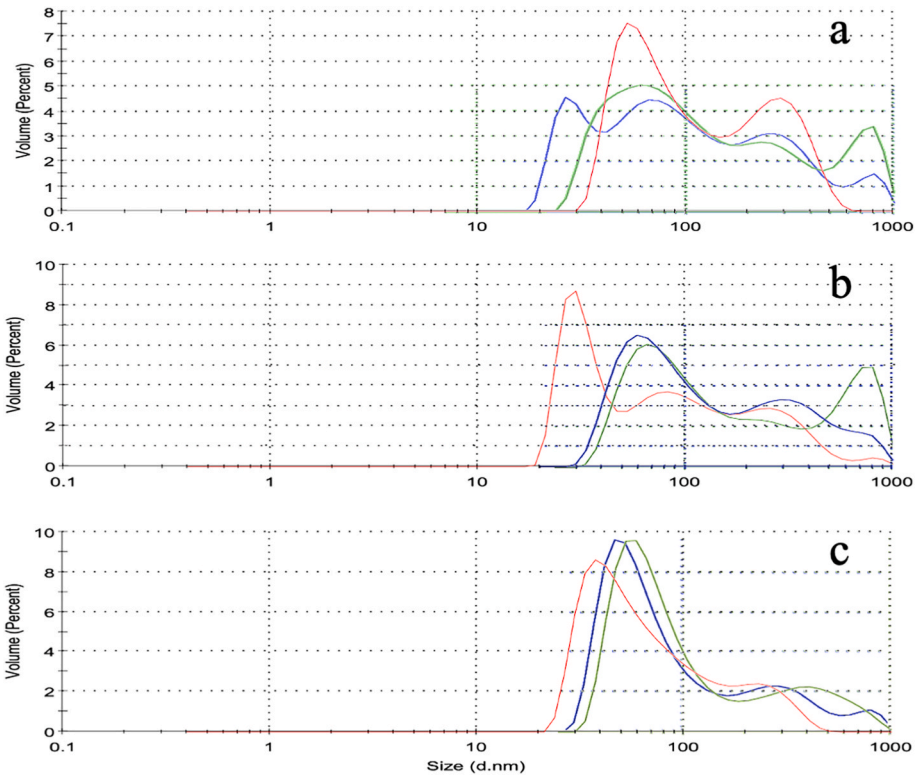

Fig. 5. Examples of Volume PSDs Measured by DLS for VLDL Samples: a) Control, b) Peroxidation, and c) Nitration

Table 6
Volume PSDs of VLDL: Mean Diameter ± SD (nm) (Relative % of Populations), n = 10.

	Population 1	Population 2	Population 3
Control	66 ± 14 (51 ± 9 %)	212 ± 112 (26 ± 16 %)	319 ± 93 (26 ± 12 %)
Peroxidation	73 ± 24 (44 ± 16 %)	230 ± 99 (31 ± 20 %)	347 ± 83 (26 ± 15 %)
Nitration	73 ± 9 (72 ± 9 %)	349 ± 63 (23 ± 9 %)	600 ± 133 (11 ± 6 %)

of the sample to 44 ± 16 %. Upon nitration, this population increases to a mean diameter of 73 ± 9 nm, and in contrast to peroxidation, the relative percentage of the smallest sized population increases to 72 ± 9 %. The mid-sized population following peroxidation trends slightly higher than native VLDL at 230 ± 99 nm but still overlaps substantially with native VLDL's mid-sized population (212 ± 112 nm). The same pattern appears for the largest population following peroxidation (347 ± 83 nm) when compared to native VLDL's largest population (319 ± 93).

The nitration reaction delivers more profound effects on the VLDL populations (Table 6). Nitration results in a decrease in the relative percentages of the mid-sized and the largest populations. The mid-sized population's average diameter increases to 349 ± 63 nm, which is 4x the average diameter of the smaller native VLDL and on its higher end 1.5x the average diameter of the mid-sized native VLDL. This indicates that VLDL could be aggregating at different stoichiometries. The largest population of native VLDL has a mean diameter of 319 ± 93 nm at a relative percentage of 26 ± 12 %. upon nitration, this population increases in size dramatically at a lower relative percentage: 600 ± 133 nm (11 ± 6 %). This population could represent aggregates of 9 of the small VLDL as well as 3 of the mid-sized VLDL particles and various combinations of the diverse VLDL particles.

In fact, Guha et al. observed that VLDL oxidation results in proteolysis, fission, fusion and rupture of particles. An increase in smaller VLDL particles indicates fission, where VLDL extrudes smaller particles that resemble HDL. Larger VLDL populations result from fusion based on proteins that crosslink between particles. These patterns are highly dependent on the type of chemical oxidation reaction and the extent of time for the reaction to take place [7]. The aggregations in the size distributions we observe for LDL and VLDL could be attributed to surface protein (apoB-100) modification and crosslinking as it has been seen in other studies [7,44].

3.4. Size distributions of clinical sample lipoproteins via dynamic light scattering

We demonstrate the feasibility of our protocol for analyzing size distribution in a clinical serum sample following the isolation of HDL, LDL, and VLDL fractions through dextran sulfate based precipation followed by ultracentrifugal flotation. The measured diameters for HDL, LDL, and VLDL from the Volume PSDs for this clinical sample were 10.82 ± 3.51 nm, 19.93 ± 6.13 nm, and 54.22 ± 7.12 nm, respectively, as shown in Fig. 6. These lipoproteins exhibited no polydispersity in contrast to the commercial lipoproteins, as they represent baseline measurements without further biochemical modifications and were derived from a single donor, unlike the also unlike the commercial lipoproteins described earlier.

Size distribution analysis via DLS is suitable for lipoproteins collected via various methods including sequential ultracentrifugal flotation and gel chromatography, which has been demonstrated before [12,21]. Clinical serum samples, such as the one analyzed here, would require a larger starting volume to facilitate additional comparative biochemical assays such as the peroxidation and nitration reactions to assess potential changes in size distribution compared to the commercial lipoproteins. However, the protein concentrations in the collected lipoprotein fractions were not sufficient to allow further subdivision for separate assays.

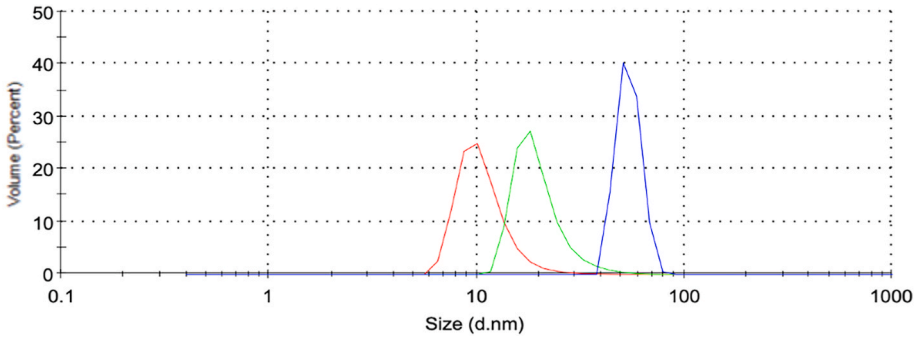

Fig. 6. Overlay of volume PSDs measured by DLS for clinical sample lipoprotein fractions: HDL (red), LDL (green), and VLDL (blue).

4. Conclusions

In this report, we demonstrate significant differences in the impact of peroxidation and nitration on lipoproteins, particularly in the formation of conjugated dienes and size distributions measured by DLS. DLS, as a method, can reveal interesting patterns of lipoprotein aggregation and fission [7,44–46] The shifts in size distributions suggest that peroxidation and nitration promote the formation of larger, aggregated particles, particularly in LDL, where substantial increases in larger populations were observed. VLDL exhibits a more complex response, with both fission and fusion events likely contributing to the observed size distribution changes.

Overall, the findings highlight the differential susceptibility of lipoprotein classes to biochemical oxidative modifications. The aggregation patterns observed here through DLS are consistent with previous studies [7,44–46] The, suggesting that the observed changes are important and further implicate oxidized lipoproteins in CVD pathogenesis. Our results underscore the need for further investigation into the specific molecular mechanisms driving lipoprotein aggregation and the potential impact on atherogenesis. Understanding the factors that drive or inhibit lipoprotein aggregation or fission can help identify innovative therapeutic approaches to slow or prevent these harmful reactions.

It may also be possible in the future to utilize DLS to measure changes in LDL particle diameter as a clinical marker of LDL peroxidation or nitration, providing valuable insights into oxidative damage and disease progression. In our previous work, we demonstrated the feasibility of using DLS to examine size distributions of clinical human samples collected via immunoseparation [13] For serum lipoproteins collected through other isolation methods, DLS could be similarly employed. For example, we demonstrate here that DLS is effective for analyzing clinical lipoprotein fractions isolated using a dextran sulfate-based precipitation assay (Cell Biolabs), which selectively separates LDL/VLDL and HDL fractions without the need for ultracentrifugation. To further refine the fractions, LDL was separated from VLDL via ultracentrifugal flotation. Using this isolation approach, we successfully obtained Volume PSDs for each lipoprotein fraction through DLS analysis. However, for future studies, the sample volume poses a limitation, as 1 mL of clinical serum does not provide sufficient protein concentration to perform both the biochemical modification assays described in this report and baseline size distribution measurements. Despite this limitation, we have demonstrated the feasibility of the approach, which may be used in the future.

Care must be taken with complex samples, as excessive polydispersity can result in low-quality measurements flagged by the DLS instrument, rendering the results uninterpretable. Lipoproteins, particularly the larger subtypes of LDL and VLDL, vary in size across the human population, and changes in their size distributions may offer more nuanced insights at the individual level compared to population-based markers like total cholesterol or non-HDL cholesterol. Similar to apolipoprotein profiling, another emerging marker of CVD risk, clinical utility for this methodology might be better suited for personalized or precision medicine approaches in future work [49] As such, future work should explore the use of DLS with consistent isolation and processing methods, such as immunoseparation or alternative techniques, to balance sample complexity with analytical reliability. This could help establish DLS as a valuable tool for monitoring biochemical changes in an individual patient's lipoproteins over the course of treatment, advancing its potential as a clinical marker for disease progression within the framework of precision medicine.

In this report we show that DLS provides us with an inexpensive, easy to implement bioanalytical tool to examine the chemical oxidation effects on lipoprotein diameters, aggregation and changes in polydispersity in solution as a first line of investigation. The sample preparation for DLS measurements is straightforward and less labor-intensive than other techniques. In contrast, techniques like electron cryomicroscopy and X-ray crystallography provide more detailed 3D images but require expensive equipment, high-quality and time-sensitive sample preparation, such as freezing for cryomicroscopy or crystallization for X-ray diffraction, as well as complex computational data analysis. These methods offer valuable structural insights and can complement DLS as a screening tool to support pharmaceutical development in future investigations. As we and several other research groups have previously demonstrated, DLS is an excellent analytical tool for examination of different facets of human lipoprotein biochemistry [12,13,21–23]. As such, DLS has the potential to add to our approach and basic biochemical understanding of the changes to lipoprotein structure paving the way for the development of therapies targeting the studied pathogenic reactions.

CRediT authorship contribution statement

Nickolette Kong: Methodology, Investigation, Conceptualization. **Natalia Penaloza:** Methodology, Investigation, Conceptualization. **Gustavo Agreda:** Writing – original draft, Investigation, Formal analysis. **Angela B. Nguyen:** Investigation, Conceptualization. **Joseph Gutheinz:** Investigation, Conceptualization. **Alison Tran:** Methodology, Conceptualization. **Nhi Nguyen:** Methodology, Investigation, Conceptualization. **Tuong Vi Ho:** Investigation. **Ana Marin:** Writing – original draft, Investigation. **Birgit Mellis:** Writing – review & editing, Writing – original draft, Formal analysis. **Richa Chandra:** Writing – review & editing, Writing – original draft, Supervision, Project administration, Methodology, Investigation, Funding acquisition, Formal analysis, Conceptualization.

Declaration of competing interest

The authors declare that they have no known competing financial interests or personal relationships that could have appeared to influence the work reported in this paper.

Acknowledgements

This work was supported in part by a Departmental Research Grant from the Welch Foundation, Grant Number AV- 0024 and in part by the Department of Education MSEIP, award number P120A200089.

Appendix A. Supplementary data

Supplementary data to this article can be found online at https://doi.org/10.1016/j.bbrep.2025.101945.

References

[1] S.S. Martin, A.W. Aday, Z.I. Almarzooq, C.A.M. Anderson, P. Arora, C.L. Avery, C. M. Baker-Smith, B. Barone Gibbs, A.Z. Beaton, A.K. Boehme, Y. Commodore-Mensah, M.E. Currie, M.S.V. Elkind, K.R. Evenson, G. Generoso, D.G. Heard, S. Hiremath, M.C. Johansen, R. Kalani, D.S. Kazi, D. Ko, J. Liu, J.W. Magnani, E. D. Michos, M.E. Mussolino, S.D. Navaneethan, N.I. Parikh, S.M. Perman, R. Poudel, M. Rezk-Hanna, G.A. Roth, N.S. Shah, M.P. St-Onge, E.L. Thacker, C.W. Tsao, S. M. Urbut, H.G.C. Van Spall, J.H. Voeks, N.Y. Wang, N.D. Wong, S.S. Wong, K. Yaffe, L.P. Palaniappan, 2024 Heart Disease and Stroke Statistics: A Report of US and Global Data from the American Heart Association, 2024, https://doi.org/10.1161/CIR.0000000000001209.

[2] M. Lu, O. Gursky, Aggregation and fusion of low-density lipoproteins in vivo and in vitro, Biomol. Concepts 4 (2013) 501–518, https://doi.org/10.1515/bmc-2013-0016.

[3] B.W. Shen, A.M. Scanu, F.J. Kezdy, Structure of human serum lipoproteins inferred from compositional analysis, Proc. Natl. Acad. Sci. U. S. A. 74 (1977) 837–841, https://doi.org/10.1073/pnas.74.3.837.

[4] M.C. Phillips, High density lipoprotein structure, Front. Biosci. 8 (2003) 1077, https://doi.org/10.2741/1077.

[5] S. Baldi, S. Frascerra, E. Ferrannini, A. Natali, LDL resistance to oxidation: effects of lipid phenotype, autologous HDL and alanine, Clin. Chim. Acta 379 (2007) 95–100, https://doi.org/10.1016/j.cca.2006.12.019.

[6] E.A. Ivanova, V.A. Myasoedova, A.A. Melnichenko, A.V. Grechko, A.N. Orekhov, Small dense low-density lipoprotein as biomarker for atherosclerotic diseases, Oxid. Med. Cell. Longev. 2017 (2017) 1273042, https://doi.org/10.1155/2017/1273042.

[7] M. Guha, O. Gursky, Effects of oxidation on structural stability and remodeling of human very low density lipoprotein, Biochemistry 49 (2010) 9584–9593, https://doi.org/10.1021/bi101391z.

[8] C.J. Packard, J. Shepherd, Lipoprotein heterogeneity and apolipoprotein B metabolism. http://ahajournals.org, 1997.

[9] J. Tejero, S. Shiva, M.T. Gladwin, Sources of vascular nitric oxide and reactive oxygen species and their regulation, Physiol. Rev. 99 (2019) 311–379, https://doi.org/10.1152/physrev.00036.2017.

[10] O.M. Panasenko, K. Briviba, L.O. Klotz, H. Sies, Oxidative modification and nitration of human low-density lipoproteins by the reaction of hypochlorous acid with nitrite, Arch. Biochem. Biophys. 343 (1997) 254–259, https://doi.org/10.1006/abbi.1997.0171.

[11] O.M. Panasenko, S.A. Evgina, E.S. Driomina, V.S. Sharov, V.I. Sergienko, Y. A. Vladimirov, Hypochlorite induces lipid peroxidation in blood lipoproteins and phospholipid liposomes, Free Radic. Biol. Med. 19 (1995) 133–140, https://doi.org/10.1016/0891-5849(94)00211-2.

[12] T. Sakurai, S. Trirongjitmoah, Y. Nishibata, T. Namita, M. Tsuji, S.P. Hui, S. Jin, K. Shimizu, H. Chiba, Measurement of lipoprotein particle sizes using dynamic light scattering, Ann. Clin. Biochem. 47 (2010) 476–481, https://doi.org/10.1258/acb.2010.010100.

[13] R. Chandra, B. Mellis, K. Garza, S.A. Hameed, J.M. Jurica, A.V. Hernandez, M. N. Nguyen, C.K. Mittal, Remnant lipoprotein size distribution profiling via dynamic light scattering analysis, Clin. Chim. Acta 462 (2016) 6–14, https://doi.org/10.1016/j.cca.2016.08.012.

[14] B.N. Khlebtsov, N.G. Khlebtsov, On the measurement of gold nanoparticle sizes by the dynamic light scattering method, Colloid J. 73 (2011) 118–127, https://doi.org/10.1134/S1061933X11010078.

[15] S.K. Brar, M. Verma, Measurement of nanoparticles by light-scattering techniques, TrAC, Trends Anal. Chem. 30 (2011) 4–17, https://doi.org/10.1016/j.trac.2010.08.008.

[16] B.J. Berne, R. Pecora, Dynamic Light Scattering: with Applications to Chemistry, Biology, and Physics, Dover, 2000.

[17] J. Stetefeld, S.A. McKenna, T.R. Patel, Dynamic light scattering: a practical guide and applications in biomedical sciences, Biophys Rev 8 (2016) 409–427, https://doi.org/10.1007/s12551-016-0218-6.

[18] I.Y. Kim, M. Kwak, J. Kim, T.G. Lee, M.B. Heo, Comparative study on nanotoxicity in human primary and cancer cells, Nanomaterials 12 (2022), https://doi.org/10.3390/nano12060993.

[19] S. Trirongjitmoah, K. Iinaga, T. Sakurai, H. Chiba, M. Sriyudthsak, K. Shimizu, Practical technique to quantify small, dense low-density lipoprotein cholesterol using dynamic light scattering, Opt. Rev. 23 (2016) 265–272, https://doi.org/10.1007/s10043-016-0187-9.

[20] T. Sakurai, S. Trirongjitmoah, Y. Nishibata, T. Namita, M. Tsuji, S.P. Hui, S. Jin, K. Shimizu, H. Chiba, Measurement of lipoprotein particle sizes using dynamic light scattering, Ann. Clin. Biochem. 47 (2010) 476–481, https://doi.org/10.1258/acb.2010.010100.

[21] S. Trirongjitmoah, K. Iinaga, T. Sakurai, H. Chiba, M. Sriyudthsak, K. Shimizu, Practical technique to quantify small, dense low-density lipoprotein cholesterol using dynamic light scattering, Opt. Rev. 23 (2016) 265–272, https://doi.org/10.1007/s10043-016-0187-9.

[22] J.E. Chatterton, P. Schlapfer, E. Bmer, M.M. Gutierrez, D.L. Puppione, C. R. Pullinger, J.P. Kane, L.K. Curtiss, V.N. Schumaker, Identification of Apolipoprotein B100 Polymorphisms that Affect Low-Density Lipoprotein Metabolism: Description of a New Approach Involving Monoclonal Antibodies and Dynamic Light Scattering1,ˆ, 1995. https://pubs.acs.org/sharingguidelines.

[23] F. Alexandre, V.H.S. Zago, N.B. Panzoldo, E.S. Parra, D.Z. Scherrer, F. Vendrame, V.S. Nunes, E.I.L. Gomes, P.D. Marcato, E.R. Nakandakare, E.C.R. Quintão, E.C. de Faria, Reference values for high-density lipoprotein particle size and volume by dynamic light scattering in a Brazilian population sample and their relationships with metabolic parameters, Clin. Chim. Acta 442 (2015) 63–72, https://doi.org/10.1016/j.cca.2015.01.006.

[24] The Scattering of Light and Other Electromagnetic Radiation - Milton Kerker - Google Books, (n.d.). https://books.google.com/books/about/The_Scattering_of_Light_and_Other_Electr.html?id=FqhmDAAAQBAJ (accessed September 9, 2024).

[25] W. Tscharnuter, Photon correlation spectroscopy in particle sizing, in: Encyclopedia of Analytical Chemistry, John Wiley & Sons, Ltd, Chichester, UK, 2000, pp. 5469–5485, https://doi.org/10.1002/9780470027318.a1512.

[26] M. Kuno, Introductory nanoscience: physical and chemical concepts, MRS Bull. 37 (2012) 405–406, https://doi.org/10.1557/mrs.2012.46.

[27] D. Langevin, E. Raspaud, S. Mariot, A. Knyazev, A. Stocco, A. Salonen, A. Luch, A. Haase, B. Trouiller, C. Relier, O. Lozano, S. Thomas, A. Salvati, K. Dawson, Towards reproducible measurement of nanoparticle size using dynamic light scattering: important controls and considerations, NanoImpact 10 (2018) 161–167, https://doi.org/10.1016/J.IMPACT.2018.04.002.

[28] E. Tomaszewska, K. Soliwoda, K. Kadziola, B. Tkacz-Szczesna, G. Celichowski, M. Cichomski, W. Szmaja, J. Grobelny, Detection limits of DLS and UV-Vis spectroscopy in characterization of polydisperse nanoparticles colloids, J. Nanomater. 2013 (2013), https://doi.org/10.1155/2013/313081.

[29] U. Kreibig, Hundert Jahre Mie-Theorie, Optische Eigenschaften von Nanopartikeln, Physik in Unserer Zeit, vol. 39, 2008, pp. 281–287, https://doi.org/10.1002/piuz.200801185.

[30] G. Mie, Beitaege zur Optik trueber Medien, speziell kolloidaler Metalloesungen, Ann. Phys. 330 (1908) 377–445.

[31] T. Moore, Absorption and scattering of light by small particles, in: C.F. Bohren, D. R. Huffman (Eds.), Wiley Science Paperback Series, 1998, https://doi.org/10.1017/S0263574798270858. Chichester, UK, 1998, xiv+530 pp., List of references, index (£34.95; pbk).

[32] M. Son, Y.S. Lee, M.J. Lee, Y.K. Park, H.R. Bae, S.Y. Lee, M.G. Shin, S. Yang, Effects of osmolality and solutes on the morphology of red blood cells according to three-dimensional refractive index tomography, PLoS One 16 (2021), https://doi.org/10.1371/journal.pone.0262106.

[33] O.M. Panasenko, S.A. Evgina, E.S. Driomina, V.S. Sharov, V.I. Sergienko, Y. A. Vladimirov, Hypochlorite induces lipid peroxidation in blood lipoproteins and phospholipid liposomes, Free Radic. Biol. Med. 19 (1995) 133–140, https://doi.org/10.1016/0891-5849(94)00211-2.

[34] M. Valko, C.J. Rhodes, J. Moncol, M. Izakovic, M. Mazur, Free radicals, metals and antioxidants in oxidative stress-induced cancer, Chem. Biol. Interact. 160 (2006) 1–40, https://doi.org/10.1016/j.cbi.2005.12.009.

[35] S. Jayaraman, D.L. Gantz, O. Gursky, Effects of oxidation on the structure and stability of human low-density lipoprotein, Biochemistry 46 (2007) 5790–5797, https://doi.org/10.1021/bi700225a.

[36] C.-Y. Han, Y. Kim Pak, Oxidation-dependent effects of oxidized LDL: proliferation or cell death, Exp. Mol. Med. 31 (1999) 165–173, https://doi.org/10.1038/emm.1999.27.

[37] J. Aguilar Diaz De Leon, C.R. Borges, Evaluation of oxidative stress in biological samples using the thiobarbituric acid reactive substances assay, JoVE J. 2020 (2020), https://doi.org/10.3791/61122.

[38] O.M. Panasenko, I.V. Gorudko, A.V. Sokolov, Hypochlorous acid as a precursor of free radicals in living systems, Biochemistry (Mosc.) 78 (2013) 1466–1489, https://doi.org/10.1134/s0006297913130075.

[39] N. Hashimoto, K. Doki, S. Kawano, K. Aonuma, M. Ieda, M. Homma, Increased serum amiodarone concentration in hypertriglyceridemic patients: effects of drug distribution to serum lipoproteins, Clin Transl Sci 15 (2022) 771–781, https://doi.org/10.1111/cts.13199.

[40] J. Aguilar Diaz De Leon, C.R. Borges, Evaluation of oxidative stress in biological samples using the thiobarbituric acid reactive substances assay, JoVE J. 2020 (2020), https://doi.org/10.3791/61122.

[41] H. Kosugi, K. Kikugawa, Potential thiobarbituric acid-reactive substances in peroxidized lipids, Free Radic. Biol. Med. 7 (1989) 205–207.

[42] G.E. Ronsein, T. Vaisar, Deepening our understanding of HDL proteome, Expert Rev. Proteomics 16 (2019) 749–760, https://doi.org/10.1080/14789450.2019.1650645.

[43] J.J. Zheng, J.K. Agus, B.V. Hong, X. Tang, C.H. Rhodes, H.E. Houts, C. Zhu, J. W. Kang, M. Wong, Y. Xie, C.B. Lebrilla, E. Mallick, K.W. Witwer, A.M. Zivkovic, Isolation of HDL by sequential flotation ultracentrifugation followed by size exclusion chromatography reveals size-based enrichment of HDL-associated proteins, Sci. Rep. 11 (2021) 1–15, https://doi.org/10.1038/s41598-021-95451-3.

[44] D.F. Meyer, M.O. Mayans, P.H.E. Groot, K.E. Suckling, K.R. Bruckdorfer, S. J. Perkins, Time-course studies by neutron solution scattering and biochemical

assays of the aggregation of human low-density lipoprotein during Cu2+-induced oxidation, Biochem. J. 310 (1995) 417–426, https://doi.org/10.1042/bj3100417.
[45] I. Maor, T. Hayek, R. Coleman, M. Aviram, Plasma LDL oxidation leads to its aggregation in the atherosclerotic apolipoprotein E-deficient mice, Arterioscler. Thromb. Vasc. Biol. 17 (1997) 2995–3005, https://doi.org/10.1161/01.ATV.17.11.2995.
[46] D.F. Meyer, A.S. Nealis, K.R. Bruckdorfer, S.J. Perkins, Characterization of the structure of polydisperse human low-density lipoprotein by neutron scattering, Biochem. J. 310 (1995), https://doi.org/10.1042/bj3100407.
[47] C.J. Packard, J. Shepherd, Lipoprotein heterogeneity and apolipoprotein B metabolism. http://ahajournals.org, 1997.
[48] J.B. German, J.T. Smilowitz, A.M. Zivkovic, Lipoproteins: when size really matters, Curr. Opin. Colloid Interface Sci. 11 (2006) 171–183, https://doi.org/10.1016/j.cocis.2005.11.006.
[49] L. Renee Ruhaak, A. van der Laarse, C.M. Cobbaert, Apolipoprotein profiling as a personalized approach to the diagnosis and treatment of dyslipidaemia, Ann. Clin. Biochem. 56 (2019) 338–356, https://doi.org/10.1177/0004563219827620.